

Article

Nonlinear Model Predictive Control for a Dynamic Positioning Ship Based on the Laguerre Function

Xiaobin Qian ^{1,2} , Helong Shen ^{2,*} , Yong Yin ² and Dongdong Guo ² 

¹ Zhilong (Dalian) Marine Technology Co., Ltd., 11th Floor, No. 523 Huangpu Road, Dalian 116020, China; qianxiaobin@zlonmarine.com

² Key Laboratory of Marine Dynamic Simulation and Control, Department of Navigation, Dalian Maritime University, Dalian 116026, China; bushyin@dlmu.edu.cn (Y.Y.); guodd2020@dlmu.edu.cn (D.G.)

* Correspondence: shenhelong@dlmu.edu.cn

Abstract: In this paper, we present a novel nonlinear model predictive control (NMPC) algorithm based on the Laguerre function for dynamic positioning ships to solve the problems of input saturation, unknown time-varying disturbances, and heavy computation. The nonlinear model of a dynamic positioning ship is presented as a linear model, transformed from a standard affine nonlinear state-space model by precise feedback linearization. The environmental disturbance is overcome using an integrator. The time cost of the proposed nonlinear control algorithm is decreased by inducing the Laguerre function to describe the feedback-linearization system input increments. The Laguerre function reduces the matrix dimensions of the nonlinear optimization problem. The simulation results for a DP supply vessel showed that the novel algorithm maintained the effective control performance of the original nonlinear model predictive control algorithm and had a reduced computation load to satisfy the requirements of real-time operation.

Keywords: dynamic positioning; input saturation; nonlinear model predictive control; Laguerre function; low computation cost



Citation: Qian, X.; Shen, H.; Yin, Y.; Guo, D. Nonlinear Model Predictive Control for a Dynamic Positioning Ship Based on the Laguerre Function. *J. Mar. Sci. Eng.* **2024**, *12*, 294. <https://doi.org/10.3390/jmse12020294>

Academic Editor: Sergei Chernyi

Received: 28 December 2023

Revised: 21 January 2024

Accepted: 4 February 2024

Published: 7 February 2024



Copyright: © 2024 by the authors. Licensee MDPI, Basel, Switzerland. This article is an open access article distributed under the terms and conditions of the Creative Commons Attribution (CC BY) license (<https://creativecommons.org/licenses/by/4.0/>).

1. Introduction

According to definitions provided by the International Maritime Organization (IMO) and Det Norske Veritas (DNV), a dynamic positioning system (DPS) comprises all the necessary equipment for a dynamic positioning ship, including the power, propulsion, and dynamic positioning control systems [1,2]. Dynamic positioning systems have been widely used in marine engineering fields such as offshore oil and gas resource development and submarine pipeline laying. Shatto [3] created the first dynamic positioning system in 1961, equipped with four steering propellers. The first DPS was employed by the ship “Cuss 1” in the California Sea. In the same year, the drillship “Eureka” [3], belonging to the Royal Dutch Shell company, was equipped with the first analog-signal DP system. The first digital-signal DP ship, “Gloma Challenger” [3], was built in 1968 and traveled almost every ocean on Earth, providing a wealth of favorable evidence for geological discoveries, especially for the theory of plate and shell structures. Subsequently, the application of microwave position reference, underwater acoustic position reference, satellite positioning, and other position reference systems improved the accuracy of dynamic positioning systems.

The dynamic position control algorithm is the key component of a DPS. The first generation of dynamic positioning systems used conventional proportional–integral–derivative (PID) control laws. To avoid responding to high-frequency movements, low-pass or notch filters were employed to eliminate high-frequency components from the deviation signal [4].

In the mid-1970s, Balchen and others proposed the use of optimal control and Kalman filtering theory combined with dynamic positioning control, giving rise to the second generation of dynamic positioning systems, which were also widely applied [5–7]. Currently, the

third generation of dynamic positioning systems focuses on advanced control algorithms such as nonlinear control algorithms and intelligent control theories [8–11]. Tannuri [12] designed a control algorithm for dynamic positioning systems based on sliding mode control and employed nonlinear multi-variable mathematical models, providing robustness to variations in displacement and environmental conditions. Do [13] developed a globally robust and adaptive output feedback controller for the dynamic positioning of surface ships under environmental disturbances based on Lyapunov's direct method, forcing the ship's position and orientation to globally asymptotically converge to the desired values. Hassani [14] proposed a new strategy for the design of robust DP controllers for marine vessels under different sea conditions using mixed- μ synthesis. Yang [15] proposed a robust adaptive NN-based output feedback control scheme for a dynamic positioning ship with uncertainties and unknown external disturbances. Zhang [16] developed a dynamic event-triggered mechanism for dynamic positioning vehicles with input saturation suited to marine applications due to its concision and flexibility. Cho [17] presented a sliding mode control algorithm as a robust dynamic positioning control technique applicable to various tasks in the marine industry.

Due to the influence of the mechanical performance of the thrusters, the control force and torque generated by a dynamic positioning system are subject to amplitude and increment constraints, i.e., the system inputs and their rates of change present saturation issues. The model predictive control (MPC) algorithm is the only advanced technology that can handle the online optimization control of multi-variable constrained systems in a systematic and intuitive manner [18], achieving favorable performance and robustness. Wang Yuanhui et al. [19], drawing inspiration from GreenDP, designed a dynamic positioning controller combining the Kalman filter and model predictive control. Subsequently [20], they used correlation-based non-switching analytical model predictive control theory to design a nonlinear model predictive controller for dynamic positioning, addressing the nonlinear control problem of dynamic positioning ship motion. Veksler [21] adopted the MPC algorithm to combine positioning control and thrust allocation into a single algorithm that could theoretically yield a near-optimal controller output. Miller [22] used the MPC regulator to control the LNG carrier training service ship "Dorchester Lady" and proved that a predictive controller could be built to steer an SS during an UNREP maneuver. However, its application was difficult due to the requirement of a ship dynamics' linear incremental model. Based on this, Miller [23] combined the MPC algorithm with the line-of-sight (LOS) approach to control Maritime Autonomous Surface Ships (MASSs) through the ship trajectory tracking system. This was combined with a variable maneuver path advance, leading to effective trajectory tracking on turns and built-in integral action reference correlation. However, the above methods only considered the thrust amplitude constraints generated by the thrusters, ignoring the constraints on the thrust amplitude increment within a certain time and non-zero-mean disturbance issues.

Model predictive control (MPC) systematically and intuitively determines the current optimal control actions based on given constraints and performance requirements. However, it faces the challenge of substantial online computations. Liuping Wang [24] proposed a discrete model predictive control method using the Laguerre function to describe the control increment signal, thereby reducing the computational load of the algorithm. Kong Xiaobing et al. [25] introduced a nonlinear model predictive control algorithm based on input-output feedback linearization, employing an approximate optimization method to reduce the online computation load of solving nonlinear constrained problems in sequential quadratic programming during the rolling optimization process.

To address the nonlinear nature of dynamic positioning ship motion, the saturation of input amplitudes and their rates of change, and the susceptibility to disturbances from the marine environment, a novel nonlinear model predictive control algorithm for the dynamic positioning of ships is proposed based on the Laguerre function. Compared to the original algorithm, this new approach effectively reduces the online computational load

while retaining control performance. It allows a ship to rapidly reach and maintain the desired position in real time.

This paper is organized as follows: Section 2 describes the problem and provides background knowledge. Section 3 presents the design process of the dynamic positioning controller and an analysis of the computation load. In Section 4, we provide simulation results demonstrating the effective performance of the proposed DP controller. Section 5 concludes the paper.

2. Problem Description and Preliminaries

This section describes the nonlinear control problem of a DP ship and introduces several key lemmas for developing the formation control strategy.

2.1. Problem Statement

A motion model of a dynamic positioning vessel at sea can be divided into low-frequency and high-frequency motions. The former describes the low-frequency motion generated by external environmental disturbances, such as low-frequency wind, second-order wave forces, and ocean currents. The latter is associated with the high-frequency motion of the vessel caused by high-frequency wind and first-order wave forces. To reduce fuel consumption and propulsion equipment wear, typically only the low-frequency motion of dynamic positioning vessels is considered, focusing on the control of horizontal motion in three degrees of freedom: surge, sway, and yaw.

In Figure 1, vector $\eta = [x, y, \psi]^T$ represents the position and heading of the vessel in the north-east coordinate system $O_0X_0Y_0$, and vector $v = [u, v, r]^T$ represents the horizontal velocity and yaw angular velocity of the vessel in the body-fixed coordinate system. Referring to Fossen, the mathematical model for the low-frequency motion of a dynamic positioning vessel on the sea surface is expressed as [2]

$$\begin{cases} \dot{\eta} = R(\psi)v \\ M\dot{v} + D(v)v = \tau + \tau_{Env} \end{cases} \quad (1)$$

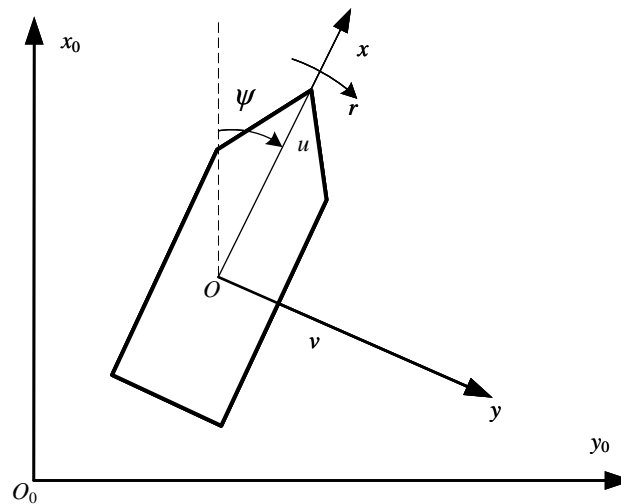


Figure 1. Horizontal coordinate frames of ship motion.

In this equation, M is the inertia matrix incorporating additional mass and is reversible and positive definite. D is the linear damping matrix, also positive definite. τ represents the actual thrust generated by the thrusters, and τ_{Env} is an unknown time-varying low-frequency disturbance term, representing the disturbing forces and moments from slowly

varying environmental disturbances such as wind, waves, and currents. R is the rotation matrix [2], expressed as

$$M = \begin{bmatrix} m_{11} & 0 & 0 \\ 0 & m_{22} & m_{23} \\ 0 & m_{32} & m_{33} \end{bmatrix} \tag{2}$$

$$R(\psi) = \begin{bmatrix} \cos \psi & -\sin \psi & 0 \\ \sin \psi & \cos \psi & 0 \\ 0 & 0 & 1 \end{bmatrix} \tag{3}$$

$$D = \begin{bmatrix} d_{11} & 0 & 0 \\ 0 & d_{22} & d_{23} \\ 0 & d_{32} & d_{33} \end{bmatrix}. \tag{4}$$

Suppose that $x = [x, y, \psi, u, v, r]^T$, $u = \tau$, $d = \tau_{Env}$, and

$$\begin{cases} \alpha_{11} = -d_{11}/m_{11} \\ \alpha_{22} = -(d_{22}m_{33} - d_{32}m_{23}) / (m_{22}m_{33} - m_{23}m_{32}) \\ \alpha_{23} = -(d_{23}m_{33} - d_{33}m_{23}) / (m_{22}m_{33} - m_{23}m_{32}) \\ \alpha_{32} = (d_{22}m_{32} - d_{32}m_{22}) / (m_{22}m_{33} - m_{23}m_{32}) \\ \alpha_{33} = (d_{23}m_{32} - d_{33}m_{22}) / (m_{22}m_{33} - m_{23}m_{32}) \end{cases} \tag{5}$$

$$\begin{cases} \beta_{11} = 2/m_{11} \\ \beta_{22} = m_{33} / (m_{22}m_{33} - m_{23}m_{32}) \\ \beta_{23} = -m_{23} / (m_{22}m_{33} - m_{23}m_{32}) \\ \beta_{32} = -m_{32} / (m_{22}m_{33} - m_{23}m_{32}) \\ \beta_{33} = m_{22} / (m_{22}m_{33} - m_{23}m_{32}) \end{cases}. \tag{6}$$

Thus, the standard nonlinear state-space model for dynamic positioning vessels is obtained as follows:

$$\begin{cases} \dot{x} = f(x) + g(x)(u + d) \\ y = h(x) \end{cases}, \tag{7}$$

where

$$f(x) = \begin{bmatrix} x_4 \cos(x_3) - x_5 \sin(x_3) \\ x_4 \sin(x_3) + x_5 \cos(x_3) \\ x_6 \\ \alpha_{11} x_4 \\ \alpha_{22} x_5 + \alpha_{23} x_6 \\ \alpha_{32} x_5 + \alpha_{33} x_6 \end{bmatrix} \tag{8}$$

$$g(x) = \begin{bmatrix} 0 & 0 & 0 \\ 0 & 0 & 0 \\ 0 & 0 & 0 \\ \beta_{11} & 0 & 0 \\ 0 & \beta_{22} & \beta_{23} \\ 0 & \beta_{32} & \beta_{33} \end{bmatrix} \tag{9}$$

$$h(x) = \begin{bmatrix} h_1(x) \\ h_2(x) \\ h_3(x) \end{bmatrix} = \begin{bmatrix} x_1 \\ x_2 \\ x_3 \end{bmatrix}. \tag{10}$$

To address the nonlinear dynamic positioning ship motion model described by Equations (1) and (7), we designed a nonlinear model predictive controller (NMPC). The goal was to enable the dynamic positioning ship to overcome environmental disturbances and reach and maintain the desired position while satisfying the system constraints.

2.2. Differential Geometry

For the control of nonlinear systems, researchers often neglect higher-order nonlinear terms by expanding the system model to a first-order linear term through Taylor expansion. However, precise feedback linearization technology uses differential geometry methods for linearization without ignoring any nonlinear terms, and the linearization of this method is accurate. To apply precise feedback linearization technology to nonlinear model predictive control, the following definition needs to be introduced.

Definition 1. If f is a smooth vector field on U and h is a smooth scalar function on U , then $f(h)$ is a smooth function on U , defined as

$$L_f h(\mathbf{x}) = \sum_{i=1}^n f_i(\mathbf{x}) \left(\frac{\partial h(\mathbf{x})}{\partial x_i} \right) \tag{11}$$

The function $L_f h$ is the Lie derivative of function h along the vector field f .

Definition 2. For a multiple input multiple output (MIMO) affine nonlinear system,

$$\begin{cases} \dot{\mathbf{x}} = \mathbf{f}(\mathbf{x}) + \mathbf{g}(\mathbf{x})\mathbf{u} \\ \mathbf{y} = \mathbf{h}(\mathbf{x}) \end{cases}, \tag{12}$$

where $\mathbf{x} \in \mathbb{R}^n$ is the n order state variables of the system. \mathbf{f} , \mathbf{g} , and \mathbf{h} are the vectors field that are sufficiently smooth on the domain $D \subset \mathbb{R}^n$. Mapping $f: D \rightarrow \mathbb{R}^n$ and $g: D \rightarrow \mathbb{R}^n$ are the vector fields in D .

For the MIMO system, there exists the integers (r_1, r_2, \dots, r_m) in the neighborhood of \mathbf{x}_0 , which satisfies that

$$L_{g_i} L_f^k h(\mathbf{x}) = 0 \begin{cases} 1 \leq j \leq m \\ 1 \leq i \leq m \\ k \leq r_i - 1 \end{cases}, \tag{13}$$

$$\boldsymbol{\alpha}(\mathbf{x}) = \begin{bmatrix} L_{g_1} L_f^{r_1-1} h_1(\mathbf{x}) & L_{g_2} L_f^{r_1-1} h_1(\mathbf{x}) & \dots & L_{g_m} L_f^{r_1-1} h_1(\mathbf{x}) \\ L_{g_1} L_f^{r_2-1} h_2(\mathbf{x}) & L_{g_2} L_f^{r_2-1} h_2(\mathbf{x}) & \dots & L_{g_m} L_f^{r_2-1} h_2(\mathbf{x}) \\ \vdots & \vdots & \ddots & \vdots \\ L_{g_1} L_f^{r_m-1} h_m(\mathbf{x}) & L_{g_m} L_f^{r_m-1} h_m(\mathbf{x}) & \dots & L_{g_m} L_f^{r_m-1} h_m(\mathbf{x}) \end{bmatrix}. \tag{14}$$

If $\boldsymbol{\alpha}(\mathbf{x})$ is the nonsingular matrix when $\mathbf{x} = \mathbf{x}_0$, the integers (r_1, r_2, \dots, r_m) are the relative degree of the output variable y_i . The total relative degree is the sum, $r = r_1 + r_2 + \dots + r_m$. If the total relative degree $r = n$, the system can achieve the precise feedback linearization.

2.3. Laguerre Function

The Laguerre functions are a class of orthogonal functions primarily used for system identification. The discrete Laguerre network is shown in Figure 2 and expressed in Equation (15) [24].

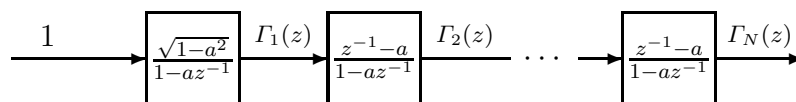


Figure 2. Discrete-time Laguerre network.

$$\Gamma_k(z) = \Gamma_{k-1}(z) \frac{z^{-1} - a}{1 - az^{-1}}, \Gamma_1(z) = \frac{\sqrt{1 - a^2}}{1 - az^{-1}}, \tag{15}$$

where a represents the poles of the discrete-time Laguerre network; the stability region is $0 \leq a \leq 1$; and N is the order of the Laguerre network. By inverse- z -transforming each

term in Equation (15), we obtain the discrete-time Laguerre functions, represented in vector form as

$$L(k) = [l_1(k) \quad l_2(k) \quad l_3(k) \quad \dots \quad l_N(k)]. \tag{16}$$

The relationship between adjacent discrete-time Laguerre functions at consecutive instants can be derived from Equations (15) and (16):

$$L(k + 1) = A_l L(k), \tag{17}$$

where the matrix A_l is a function of parameters a and β , with initial conditions

$$L(0) = \sqrt{\beta} [1 \quad -a \quad \dots (-a)^{N-1}]^T \tag{18}$$

$$A_l = \begin{bmatrix} a & 0 & 0 & \dots & 0 \\ \beta & a & 0 & \dots & 0 \\ -a\beta & \beta & a & \dots & 0 \\ \vdots & \vdots & \vdots & \ddots & \vdots \\ (-a)^{N-2}\beta & (-a)^{N-3}\beta & (-a)^{N-4}\beta & \dots & a \end{bmatrix}. \tag{19}$$

Additionally, an important property of discrete-time Laguerre functions is orthogonality [24]:

$$\begin{cases} \sum_{k=0}^{\infty} l_i(k)l_j(k) = 0, i \neq j \\ \sum_{k=0}^{\infty} l_i(k)l_j(k) = 1, i = j \end{cases}. \tag{20}$$

Based on the above properties, the impulse response of a stable system can be represented by the following discrete-time Laguerre functions:

$$H(k) = L(k)^T \bar{\eta} = L(k)^T [c_1 \quad c_2 \quad c_3 \quad \dots \quad c_N]^T, \tag{21}$$

where $\bar{\eta} = L(k)^T [c_1, c_2, c_3, \dots, c_N]$ are coefficients determined by the system data, and leveraging the orthogonality of the Laguerre functions allows one to obtain the values of each coefficient.

$$c_i = \sum_{k=0}^{\infty} H(k)l_i(k) \tag{22}$$

3. Steps for Dynamic Positioning Controller Design

3.1. Precise Feedback Linearization

The mathematical model of dynamic positioning vessel motion in Equation (7) is a standard affine nonlinear expression. Feedback linearization is required before applying the model predictive control algorithm. First, the Lie derivatives of the system output variables in Equation (7) are calculated:

$$\begin{bmatrix} L_{g_1} L_f^0 h_1 & L_{g_2} L_f^0 h_1 & L_{g_3} L_f^0 h_1 \\ L_{g_1} L_f^0 h_2 & L_{g_2} L_f^0 h_2 & L_{g_3} L_f^0 h_2 \\ L_{g_1} L_f^0 h_3 & L_{g_2} L_f^0 h_3 & L_{g_3} L_f^0 h_3 \end{bmatrix} = \begin{bmatrix} 0 & 0 & 0 \\ 0 & 0 & 0 \\ 0 & 0 & 0 \end{bmatrix} \tag{23}$$

$$a(x) = \begin{bmatrix} L_{g_1} L_f^0 h_1 & L_{g_2} L_f^0 h_1 & L_{g_3} L_f^0 h_1 \\ L_{g_1} L_f^0 h_2 & L_{g_2} L_f^0 h_2 & L_{g_3} L_f^0 h_2 \\ L_{g_1} L_f^0 h_3 & L_{g_2} L_f^0 h_3 & L_{g_3} L_f^0 h_3 \end{bmatrix} = \begin{bmatrix} \beta_{11} \cos x_3 & -\beta_{22} \sin x_3 & -\beta_{23} \sin x_3 \\ \beta_{11} \sin x_3 & \beta_{22} \cos x_3 & \beta_{23} \cos x_3 \\ 0 & \beta_{32} & \beta_{33} \end{bmatrix}. \tag{24}$$

According to Equations (23) and (24), the relative orders of the system are $r_1 = 2$, $r_2 = 2$, and $r_3 = 2$, and the total relative order $r = r_1 + r_2 + r_3$ is equal to the number of system state variables. Therefore, the nonlinear model of dynamic positioning vessel motion can undergo exact state feedback linearization, resulting in new state variables:

$$\begin{cases} x_{m_1} = L_f^0 h_1^x = x_1 \\ x_{m_2} = L_f^0 h_2^x = x_2 \\ x_{m_3} = L_f^0 h_3^x = x_3 \\ x_{m_4} = L_f^1 h_1^x = x_4 \cos(x_3) - x_5 \sin(x_3) \\ x_{m_5} = L_f^1 h_2^x = x_4 \sin(x_3) + x_5 \cos(x_3) \\ x_{m_6} = L_f^1 h_3^x = x_6 \end{cases} \quad (25)$$

The nonlinear feedback control rate is given by

$$u = a(x)^{-1}(-b(x) + v) - d, \quad (26)$$

in which

$$b(x) = \begin{bmatrix} L_f^2 h_1 \\ L_f^2 h_2 \\ L_f^2 h_3 \end{bmatrix} = \begin{bmatrix} \cos x_3 (\alpha_{11} x_4 - x_5 x_6) - \sin x_3 (\alpha_{22} x_5 + \alpha_{23} x_6 + x_4 x_6) \\ \sin x_3 (\alpha_{11} x_4 - x_5 x_6) + \cos x_3 (\alpha_{22} x_5 + \alpha_{23} x_6 + x_4 x_6) \\ \alpha_{32} x_5 + \alpha_{33} x_6 \end{bmatrix}. \quad (27)$$

The linear model obtained through feedback linearization is

$$\begin{cases} \dot{x}_m = A_c x_m + B_c v + E_c d \\ y = C_c x_m \end{cases} \quad (28)$$

The coefficients of each matrix in this equation are $A_c = \begin{bmatrix} 0 & 0 & 0 & 1 & 0 & 0 \\ 0 & 0 & 0 & 0 & 1 & 0 \\ 0 & 0 & 0 & 0 & 0 & 1 \\ 0 & 0 & 0 & 0 & 0 & 0 \\ 0 & 0 & 0 & 0 & 0 & 0 \\ 0 & 0 & 0 & 0 & 0 & 0 \end{bmatrix},$

$$B_c = \begin{bmatrix} 0 & 0 & 0 \\ 0 & 0 & 0 \\ 0 & 0 & 0 \\ 1 & 0 & 0 \\ 0 & 1 & 0 \\ 0 & 0 & 1 \end{bmatrix}, C_c = \begin{bmatrix} 1 & 0 & 0 & 0 & 0 & 0 \\ 0 & 1 & 0 & 0 & 0 & 0 \\ 0 & 0 & 1 & 0 & 0 & 0 \end{bmatrix}, E_c = B_c a(x).$$

3.2. Linear Control Structure

Discretizing the state-space model (28) with a step size of h yields the discretized linear model:

$$\begin{cases} x_m(k+1) = A_d x_m(k) + B_d v(k) + E_d d(k) \\ y(k) = C_d x_k \end{cases} \quad (29)$$

Here, $x_m(k)$ represents the state of the linear system at time k ; $v(k)$ is the input to the linear system; $y(k)$ is the output of the linear system at time k ; and $A_d, B_d, C_d,$ and E_d are the constant matrices after discretization.

Suppose that $x_m(k+1) = x_m(k) + \Delta x_m(k+1)$ and $v_m(k+1) = v_m(k) + \Delta v_m(k+1)$; then, based on Equation (29), we obtain

$$\begin{cases} \Delta x_m(k+1) = A_d \Delta x_m(k) + B_d \Delta v(k) \\ y(k+1) = y(k) + C_d (A_d \Delta x_m(k) + B_d \Delta v(k)) \end{cases} \quad (30)$$

Suppose that $x_u(k) = [\Delta x_m(k)^T, y(k)^T]^T$; introducing an integral component, we obtain an augmented state-space model that eliminates the slowly varying disturbance term d , expressed as follows:

$$\begin{cases} \mathbf{x}_u(k+1) = \mathbf{A}_u(k) + \mathbf{B}\Delta\mathbf{v}(k) \\ \mathbf{y}(k) = \mathbf{C}_d\mathbf{x}_u(k) \end{cases} \quad (31)$$

Here, \mathbf{A} , \mathbf{B} , and \mathbf{C} represent the constant augmented matrix coefficients, which are as follows: $\mathbf{A} = \begin{bmatrix} \mathbf{A}_d & \mathbf{0}_{6 \times 3} \\ \mathbf{C}_d\mathbf{A}_d & \mathbf{I}_{6 \times 3} \end{bmatrix}$, $\mathbf{B} = \begin{bmatrix} \mathbf{B}_d \\ \mathbf{C}_d\mathbf{B}_d \end{bmatrix}$, $\mathbf{C} = [\mathbf{0}_{3 \times 6} \quad \mathbf{I}_{3 \times 3}]$.

According to Equations (29) and (30), the future N_c system outputs N_p in the control time domain can be predicted as follows ($N_c \leq N_p$):

$$\mathbf{Y} = \mathbf{F}\mathbf{x}_u(k) + \Phi\Delta\mathbf{V}. \quad (32)$$

In the equation above, $\mathbf{Y} = \begin{bmatrix} \mathbf{y}(k+1|k) \\ \mathbf{y}(k+1|k) \\ \vdots \\ \mathbf{y}(k+1|k) \end{bmatrix}$, $\Delta\mathbf{V} = \begin{bmatrix} \Delta\mathbf{v}(k) \\ \Delta\mathbf{v}(k+1) \\ \vdots \\ \Delta\mathbf{v}(k+N_c-1) \end{bmatrix}$

$$\mathbf{F} = \begin{bmatrix} \mathbf{CA} \\ \mathbf{CA}^2 \\ \vdots \\ \mathbf{CA}^{N_p} \end{bmatrix}, \Phi = \begin{bmatrix} \mathbf{CB} & \mathbf{0} & \dots & \mathbf{0} \\ \mathbf{CAB} & \mathbf{CB} & \dots & \mathbf{0} \\ \vdots & \vdots & \ddots & \vdots \\ \mathbf{CA}^{N_p-1}\mathbf{B} & \mathbf{CA}^{N_p-2}\mathbf{B} & \dots & \mathbf{CA}^{N_p-N_c}\mathbf{B} \end{bmatrix}.$$

Additionally, based on Equations (26), (29), and (30), the relationship between the entire predicted time domain's linear system state variables and the input \mathbf{v} can be obtained:

$$\mathbf{X}_{mk} = \mathbf{\Gamma} + \mathbf{\Pi}\Delta\mathbf{V}, \quad (33)$$

where $\mathbf{X}_m(k) = \begin{bmatrix} \mathbf{x}_m(k) \\ \mathbf{x}_m(k+1) \\ \vdots \\ \mathbf{x}_m(k+N_c-1) \end{bmatrix}$, $\mathbf{\Gamma} = \begin{bmatrix} \mathbf{x}_m(k) \\ \mathbf{x}_m(k) + \sum_{i=1}^1 \mathbf{A}_d^i \Delta\mathbf{x}_m(k) \\ \vdots \\ \mathbf{x}_m(k) + \sum_{i=1}^{N_c-1} \mathbf{A}_d^i \Delta\mathbf{x}_m(k) \end{bmatrix}$

$$\mathbf{\Pi} = \begin{bmatrix} \mathbf{0} & \mathbf{0} & \dots & \mathbf{0} \\ \sum_{i=1}^1 (\mathbf{A}_m^{i-1})\mathbf{B}_m & \mathbf{0} & \dots & \mathbf{0} \\ \vdots & \vdots & \ddots & \vdots \\ \sum_{i=1}^{N_p-1} (\mathbf{A}_m^{i-1})\mathbf{B}_m & \sum_{i=1}^{N_p-1} (\mathbf{A}_m^{i-1})\mathbf{B}_m & \dots & \mathbf{0} \end{bmatrix}.$$

The optimization objective function is formulated as a quadratic function of $\Delta\mathbf{V}$:

$$J = (\mathbf{N}_d - \mathbf{Y})^T (\mathbf{N}_d - \mathbf{Y}) + \Delta\mathbf{V}^T \mathbf{R}_w \Delta\mathbf{V}, \quad (34)$$

where \mathbf{R}_w represents the input weight. Substituting Equation (32) into the previous expression yields the performance index J_{min} with respect to $\Delta\mathbf{V}$:

$$J_{min} = \frac{1}{2} \Delta\mathbf{V}^T \mathbf{H} \Delta\mathbf{V} + \mathbf{f}^T \Delta\mathbf{V}, \quad (35)$$

where the Hessian matrix \mathbf{H} and the vector \mathbf{f} are defined as follows:

$$\mathbf{H} = 2(\mathbf{\Phi}^T \mathbf{\Phi} + \mathbf{R}_w) \quad (36)$$

$$\mathbf{f} = -2\mathbf{\Phi}(\mathbf{N}_d - \mathbf{F}\mathbf{x}_u(k)). \quad (37)$$

Under unconstrained conditions, the optimal solution for $\Delta\mathbf{V}$ is given by

$$\Delta\mathbf{V} = (\mathbf{\Phi}^T \mathbf{\Phi} + \mathbf{R}_w)^{-1} \mathbf{\Phi}^T (\mathbf{N}_d - \mathbf{F}\mathbf{x}_u(k)). \quad (38)$$

Due to the physical limitations of the propulsion system on a dynamic positioning vessel, the total control force and moment generated by the thrusters are constrained.

Additionally, the amplitude of the total control force and moment changes within a certain time is also constrained, indicating the presence of input and input rate saturation in the system:

$$\mathbf{u}_{min}(k) \leq \mathbf{u}(k) \leq \mathbf{u}_{max}(k) \tag{39}$$

$$\Delta \mathbf{u}_{min}(k) \leq \Delta \mathbf{u}(k) \leq \Delta \mathbf{u}_{max}(k). \tag{40}$$

The input \mathbf{u} of the nonlinear dynamic positioning vessel motion model under the mapping of the nonlinear feedback control rate (26) results in the input \mathbf{v} for the new linear system. The linear inequality constraints (39) and (40) with respect to \mathbf{u} are transformed into nonlinear inequality constraints for \mathbf{v} . However, the upper and lower bounds of \mathbf{V} throughout the control time domain, \mathbf{V}_{min} and \mathbf{V}_{max} , cannot be directly determined. Their values are dependent on the system's state at each sampling moment and need to be determined. According to Equation (26), the relationship between \mathbf{U} and \mathbf{V} throughout the entire control time domain can be obtained:

$$\begin{cases} \mathbf{u}(k) = \mathbf{a}(\mathbf{x}(k))^{-1}(-\mathbf{b}(\mathbf{x}(k)) + \mathbf{v}(k)) \\ \mathbf{u}(k + 1) = \mathbf{a}(\mathbf{x}(k + 1))^{-1}(-\mathbf{b}(\mathbf{x}(k + 1)) + \mathbf{v}(k + 1)) \\ \vdots \\ \mathbf{u}(k + N_c - 1) = \mathbf{a}(\mathbf{x}(k + N_c - 1))^{-1}(-\mathbf{b}(\mathbf{x}(k + N_c - 1)) + \mathbf{v}(k + N_c - 1)) \end{cases} \tag{41}$$

That is,

$$\mathbf{U}(k) = f_{xv}(\mathbf{X}(k), \mathbf{V}(k)). \tag{42}$$

The original nonlinear system input \mathbf{u} and the linear system input \mathbf{v} can both be obtained by summing their control increments \mathbf{u} and \mathbf{v} ; that is,

$$\mathbf{u}(k + m) = \mathbf{u}(k - 1) + \Delta \mathbf{u}(k) + \dots + \Delta \mathbf{u}(k + m) \tag{43}$$

$$\mathbf{v}(k + m) = \mathbf{v}(k - 1) + \Delta \mathbf{v}(k) + \dots + \Delta \mathbf{v}(k + m). \tag{44}$$

Therefore, \mathbf{U} and \mathbf{V} over the entire control time domain are given by

$$\mathbf{U}(k) = \mathbf{C}_1 \mathbf{u}(k - 1) + \mathbf{C}_2 \Delta \mathbf{U}(k) \tag{45}$$

$$\mathbf{V}(k) = \mathbf{C}_1 \mathbf{v}(k - 1) + \mathbf{C}_2 \Delta \mathbf{V}(k), \tag{46}$$

where $\mathbf{C}_1 = \begin{bmatrix} \mathbf{I} \\ \mathbf{I} \\ \vdots \\ \mathbf{I} \end{bmatrix}$, $\mathbf{C}_2 = \begin{bmatrix} \mathbf{I} & 0 & \dots & 0 \\ \mathbf{I} & \mathbf{I} & \dots & 0 \\ \vdots & \vdots & \ddots & \vdots \\ \mathbf{I} & \mathbf{I} & \dots & \mathbf{I} \end{bmatrix}$.

Substituting the combined expressions (33) and (46) into (42) yields a nonlinear expression for \mathbf{U} in terms of $\Delta \mathbf{V}$:

$$\mathbf{U} = f_{\Delta v}(\Delta \mathbf{V}). \tag{47}$$

The constraint conditions, transformed from the linear constraints on \mathbf{U} in (39) and (40), are combined with (36) and (47) to form the following nonlinear programming problem:

$$\begin{cases} \min & J = \frac{1}{2} \Delta \mathbf{V}^T \mathbf{H} \Delta \mathbf{V} + \mathbf{f}^T \Delta \mathbf{V} \\ \text{suchthat} & \mathbf{c}(\Delta \mathbf{V}) \geq 0 \end{cases} \tag{48}$$

The left-hand side of the nonlinear constraint inequality in this equation is

$$c(\Delta V) = \begin{bmatrix} f_{\Delta v}(\Delta V) - \mathbf{U}_{max} \\ \mathbf{U}_{min} - f_{\Delta v}(\Delta V) \\ \mathbf{C}_2^{-1}(f_{\Delta v}(\Delta V) - \mathbf{C}_1 \mathbf{u}(k-1)) - \Delta \mathbf{U}_{max} \\ \Delta \mathbf{U}_{min} - \mathbf{C}_2^{-1}(f_{\Delta v}(\Delta V) - \mathbf{C}_1 \mathbf{u}(k-1)) \end{bmatrix}. \tag{49}$$

The current optimal solution for the feedback-linearized system input at time k , denoted as ΔV^{opt} , is obtained by solving the nonlinear programming problem in Equation (48) using the sequential quadratic programming method. In this process, the initial point for iteration is set according to Equation (38), and the transformed values are derived to obtain the inputs for the original nonlinear system, representing the required thrust and moments for the dynamic positioning of the ship.

$$\mathbf{u}(k) = \mathbf{a}(\mathbf{x}(k))^{-1}[\mathbf{a}(\mathbf{x}(k-1))\mathbf{u}(k-1) + \mathbf{b}(\mathbf{x}(k-1)) - \mathbf{b}(\mathbf{x}(k)) + \Delta v(k)] \tag{50}$$

3.3. Introduction to Laguerre Functions

A nonlinear model predictive control algorithm typically selects a relatively large and appropriate control horizon (N_c) to ensure a more favorable dynamic response and stability. However, increasing the control horizon also increases the solution time for the nonlinear programming problem, preventing the computer from issuing control commands in real time and affecting the positioning of the ship. Therefore, we introduce Laguerre functions to describe the control increments of the linearized system after feedback, proposing a new low-computational-cost nonlinear model predictive control algorithm for ship dynamic positioning.

We assume that the future m time steps of the linear system control input increments at the current time step k are represented by the following Laguerre function:

$$\Delta v(k+m) = \mathbf{L}(m)^T \bar{\boldsymbol{\eta}}_k, \tag{51}$$

$$\text{where } \mathbf{L}(m)^T = \begin{bmatrix} L_1(m)^T & \mathbf{0}_{1 \times N} & \mathbf{0}_{1 \times N} \\ \mathbf{0}_{1 \times N} & L_2(m)^T & \mathbf{0}_{1 \times N} \\ \mathbf{0}_{1 \times N} & \mathbf{0}_{1 \times N} & L_3(m)^T \end{bmatrix}, \bar{\boldsymbol{\eta}}_k = \begin{bmatrix} \bar{\eta}_{k_1} \\ \bar{\eta}_{k_2} \\ \bar{\eta}_{k_3} \end{bmatrix}.$$

Substituting Equation (51) into the augmented state-space model (31), we obtain a state-space model incorporating the Lagrange function:

$$\begin{cases} \mathbf{x}_u(k+1) = \mathbf{A}\mathbf{x}_u(k) + \mathbf{B}\mathbf{L}(0)^T \bar{\boldsymbol{\eta}}_k \\ \mathbf{y}(k) = \mathbf{C}\mathbf{x}(k) \end{cases}. \tag{52}$$

Thus, based on the current state and output sampled at time k , we can predict the system's state and output at future time $k+m$:

$$\mathbf{x}_u(k+m|k) = \mathbf{A}^m \mathbf{x}_u(k) + \boldsymbol{\phi}(m)^T \bar{\boldsymbol{\eta}}_k \tag{53}$$

$$\mathbf{y}(k+m|k) = \mathbf{C}\mathbf{A}^m \mathbf{x}_u(k) + \boldsymbol{\phi}(m)^T \mathbf{C}\bar{\boldsymbol{\eta}}_k, \tag{54}$$

where $\boldsymbol{\phi}(m)^T = \sum_{i=0}^{m-1} \mathbf{A}^{m-i-1} \mathbf{B}\mathbf{L}(i)^T$. Then, we substitute the Laguerre function into the optimization objective function (Equation (34)) to obtain

$$J = \sum_{m=1}^{N_p} [\boldsymbol{\eta}_d + \mathbf{y}(k+m)]^T [\boldsymbol{\eta}_d + \mathbf{y}(k+m)] + \sum_{n=0}^{N_p-1} [\mathbf{L}(n)^T \bar{\boldsymbol{\eta}}_k]^T [\mathbf{L}(n)^T \bar{\boldsymbol{\eta}}_k]. \tag{55}$$

Due to the sufficiently large prediction horizon N_p , the orthogonality of the Lagrange functions can be exploited to simplify the second term of Equation (55), resulting in

$$J = \sum_{m=1}^{N_p} [\boldsymbol{\eta}_d + \mathbf{y}(k+m)]^T [\boldsymbol{\eta}_d + \mathbf{y}(k+m)] + \bar{\boldsymbol{\eta}}_k^T \mathbf{R}_L \bar{\boldsymbol{\eta}}_k. \tag{56}$$

Introducing the variable $x_f(k) = [\Delta_m(k)^T, e(k)^T]^T$ and substituting Equations (53) and (54) into Equation (56) yields the new performance index function:

$$J = \frac{1}{2} \bar{\eta}^T \bar{H} \bar{\eta} + \bar{f}^T \bar{\eta}, \tag{57}$$

where the Hessian matrix \bar{H} and the vector \bar{f} are represented as

$$\bar{H} = 2 \left(\sum_{m=1}^{N_p} \phi(m) C^T C \phi(m)^T + R_L \right) \tag{58}$$

$$\bar{f} = 2 \sum_{m=1}^{N_p} (\phi(m) C^T C A^m) x_f(k). \tag{59}$$

Under unconstrained conditions, the optimal solution for $\bar{\eta}$ is

$$\bar{\eta}^{opt} = -\bar{H}^{-1} \bar{f}. \tag{60}$$

To handle the nonlinear constraint conditions in the original nonlinear programming problem (48), the Laguerre function must be sequentially substituted into (33), (42) and (46) to obtain the expression of \mathbf{U} in terms of $\bar{\eta}$:

$$\mathbf{U} = f_{\eta}(\bar{\eta}). \tag{61}$$

By combining Equation (57) and Equation (61), we rewrite the original nonlinear programming problem (48) in terms of ΔV , forming a new nonlinear programming problem with respect to $\bar{\eta}$:

$$\begin{cases} \min & J = \frac{1}{2} \bar{\eta}^T \bar{H} \bar{\eta} + \bar{f}^T \bar{\eta} \\ \text{suchthat} & c(\bar{\eta}) \geq 0 \end{cases}, \tag{62}$$

where

$$c(\bar{\eta}) = \begin{bmatrix} f_{\eta}(\bar{\eta}) - \mathbf{U}_{max} \\ \mathbf{U}_{min} - f_{\eta}(\bar{\eta}) \\ C_2^{-1}(f_{\eta}(\bar{\eta}) - C_1 \mathbf{u}(k-1)) - \Delta \mathbf{U}_{max} \\ \Delta \mathbf{U}_{min} - C_2^{-1}(f_{\eta}(\Delta V) - C_1 \mathbf{u}(k-1)) \end{bmatrix}. \tag{63}$$

Finally, employing the sequential quadratic programming method, the optimal solution to Equation (62) is determined, with Equation (60) used as the initial point. This provides the required thrust and torque for the current time step k in the dynamic positioning of the vessel.

$$\mathbf{u}(k) = \mathbf{a}(x(k))^{-1} [\mathbf{a}(x(k-1)) \mathbf{u}(k-1) + \mathbf{b}(x(k-1)) - \mathbf{b}(x(k)) + \mathbf{L}(0)^T \bar{\eta}_k^{opt}] \tag{64}$$

3.4. Computational Analysis

The sequential quadratic programming algorithm involves approximating the nonlinear programming function at a certain point through a Taylor expansion into multiple quadratic programming problems and iteratively obtaining the optimal solution. Its computational complexity increases exponentially with the dimensionality of the variables.

The original nonlinear model predictive control method's nonlinear optimization problem, expressed in Equation (48), and the new nonlinear optimization problem of the model predictive control algorithm based on the Laguerre function, expressed in Equation (62), have a similar form. However, the dimensions of their internal variables differ. In Equation (48), the variable ΔV has dimensions of $3N_c \times 1$, the Hessian matrix H has dimensions of $3N_c \times 3N_c$, and the coefficient vector f has dimensions of $3N_c \times 1$. Meanwhile, for the new algorithm's optimization problem (62), the variable $\bar{\eta}$ has dimensions of $3N \times 1$, the Hessian matrix \bar{H} has dimensions of $3N \times 3N$, and the coefficient vector

\bar{F} has dimensions of $3N \times 1$. In practical applications, the Laguerre function series N is much smaller than the control time domain N_c . Therefore, in the process of sequential quadratic programming, with the same number of iterations, the computational load of the proposed ship dynamic positioning nonlinear model predictive control algorithm based on the Laguerre function is reduced compared to the original algorithm.

4. Simulation Verification and Data Analysis

To validate the effectiveness of the proposed ship dynamic positioning nonlinear model predictive control algorithm based on the Laguerre function, simulation verification was conducted using a dynamic positioning supply ship as the research object. The supply ship had a length of 76.1 m, a width of 18.8 m, a draft of 6.25 m, and a displacement of 4200 t. The main parameters are detailed in Table 1, and the non-dimensional inertia matrix and damping matrix were as follows [26]:

$$M'' = \begin{bmatrix} 1.1274 & 0.0000 & 0.0000 \\ 0.0000 & 1.8902 & -0.0744 \\ 0.0000 & -0.0744 & 0.1278 \end{bmatrix} \tag{65}$$

$$D'' = \begin{bmatrix} 0.0358 & 0.0000 & 0.0000 \\ 0.0000 & 0.1183 & -0.0124 \\ 0.0000 & -0.0041 & 0.0308 \end{bmatrix}. \tag{66}$$

The simulation experiment was configured using a nonlinear model predictive controller with a prediction horizon (N_p) of 10, a control horizon (N_c) of 150, Laguerre function poles $a = [0.46, 0.46, 0.46]^T$, and a series order of $N = [4, 4, 4]^T$. The initial position of the ship was set to $\eta_0 = [0 \text{ m}, 0 \text{ m}, 30^\circ]$, and the desired position was $\eta_0 = [20 \text{ m}, 20 \text{ m}, 40^\circ]$. The low-frequency environmental disturbance was set to a certain value.

$$\tau_{Env} = R^T(\psi) \cdot \begin{bmatrix} 3(1.2 + 1.5 \sin(0.02t) + 1.4 \sin(0.1t))\text{kN} \\ 14(-0.9 + 2.0 \sin(0.02t) + 1.3 \sin(0.2t))\text{kN} \\ 250(\sin(0.09t) + 4 \sin(0.01t))\text{kN} \cdot \text{m} \end{bmatrix} \tag{67}$$

Under simulated conditions equivalent to sea state four operations, the simulation time was set to 500 s with a time step of 0.5 s. The experiment was conducted on a Lenovo desktop computer equipped with an Intel Core(TM) i7-6700 CPU running at 3.4 GHz and with 8 GB of RAM. The results of the experiment are depicted in Figures 3–8, where the blue dashed line represents the original algorithm, and the red solid line represents the new NMPC algorithm based on the Laguerre function. Additionally, the results are summarized in Table 2.

Table 1. The main parameters of the DP supply vessel.

Parameter	Value	Parameter	Value
L_{oa}	76.1 m	B_m	18.8 m
d_m	6.25 m	DWT	4200 t
X	−1000~1000 kN	Y	−300~300 kN
N	−7620~7620 kN·m	ΔX	−200~200 kN/s
ΔY	−60~60 kN/s	ΔN	−1524~1524 kN·m/s

Simulation experiment results analysis: Overall, the response curves of the proposed nonlinear model predictive control (NMPC) algorithm for ship dynamic positioning were almost identical to those of the original algorithm. Figures 3 and 4 show the ship’s trajectory and time response under low-frequency environmental disturbance, indicating that the designed controller overcame ocean environmental disturbances to bring the ship to and maintain it at the desired position. Figure 5 represents the ship’s speed response curve; the speed components had relatively small values, and, under the influence of environmental disturbances, they oscillated near the zero point. Figure 6 illustrates the response curves of

ship control forces and torques and their rate of change, showing that the control forces and torques were within the constraint range. Ultimately, they oscillated around a fixed value to counteract the impact of ocean environmental disturbances on the ship. Figure 7 represents the response curves for the rate of change in the control forces and torques, all within their constraint range, which oscillated around a zero mean. Figure 8 and Table 2 compare the computational load of the newly designed ship dynamic positioning NMPC algorithm based on the Laguerre function with that of the original algorithm. The graph indicates that the new algorithm’s single-computation time was significantly lower than that of the original algorithm. During the 1 s–17 s simulation period, the original algorithm’s single minimum computation time was 227.9 ms, with a maximum of 1847.0 ms and an average of 684.2 ms, preventing the real-time calculation of the control algorithm. During this period, the new algorithm’s single minimum computation time was 10.9 ms, the maximum was 227.9 ms, and the average was 134.6 ms, marking a decrease of 80.3% compared to the original algorithm. In the subsequent simulation period from 17 s to 500 s, as the sequential quadratic programming (SQP) iteration’s starting point was already the optimal point, the computational load was the same as when unconstrained. The new algorithm’s average computation time during this period was 13.6 ms, a 22.8% decrease compared to the original algorithm’s time of 10.5 ms. Overall, the average computation time of the new algorithm was 14.6 ms, representing a 59.1% decrease compared to the original algorithm’s time of 35.7 ms, ensuring the real-time performance of the algorithm solution.

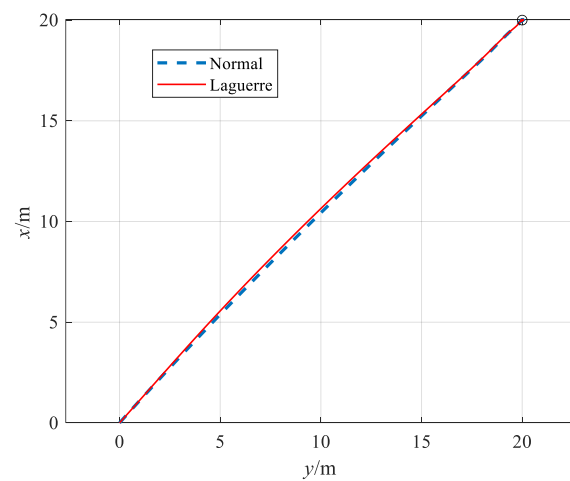


Figure 3. Response trajectory curves of the DP vessel.

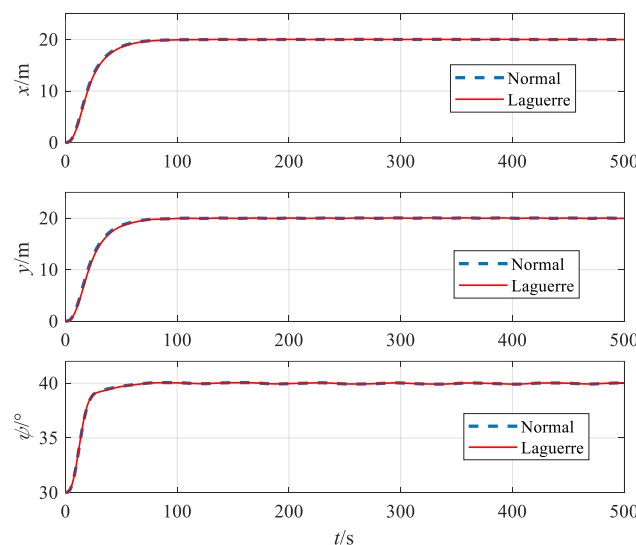


Figure 4. Response curves of positions and headings.

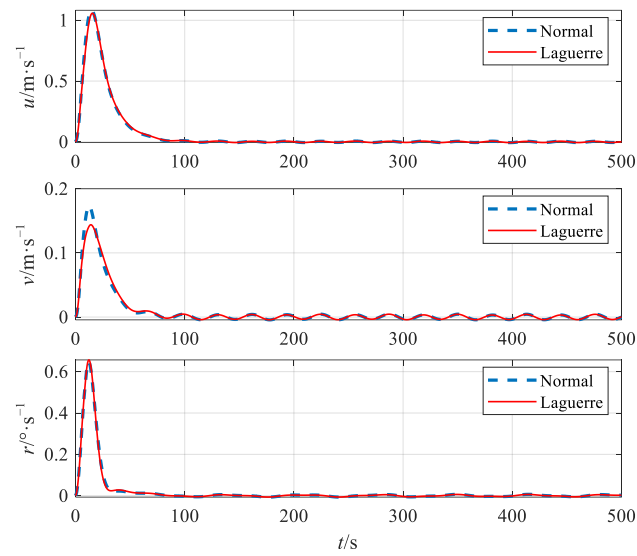


Figure 5. Response curves of ship velocity and yaw rate.

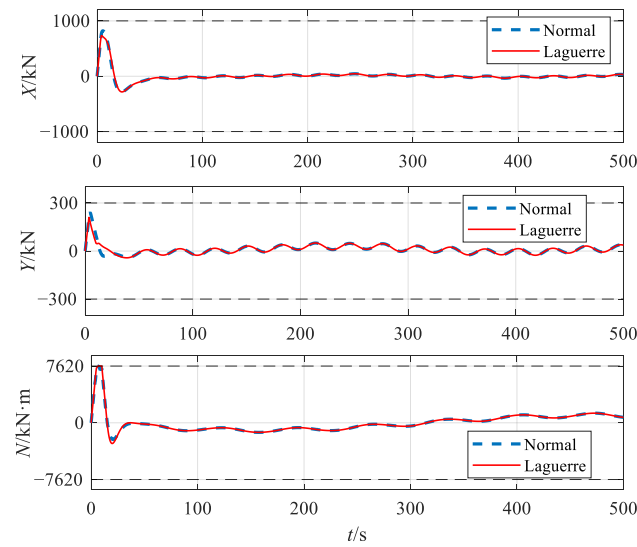


Figure 6. Response curves of control forces and moments.

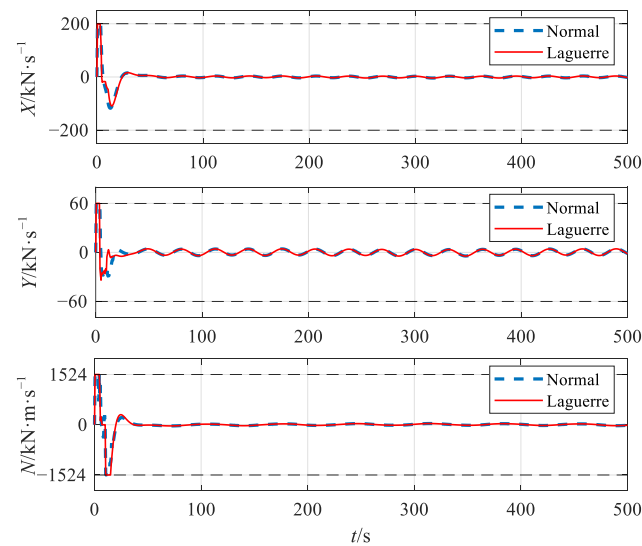


Figure 7. Response curves of control forces and moment rates.

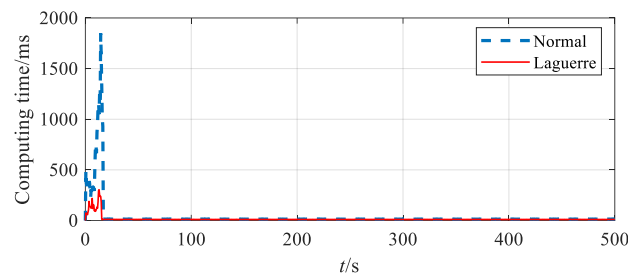


Figure 8. Comparison of computation load.

Table 2. Comparison of mean computation time.

Time Range	Mark	New Algorithm (ms)	Origin Algorithm (ms)	Difference
1 s~17 s	Min	10.9	227.9	
1 s~17 s	Max	304.4	1847.0	
1 s~17 s	Mean	134.6	684.2	80.3%
17 s~500 s	Min	10.1	13.1	
17 s~500 s	Max	12.3	15.9	
17 s~500 s	Mean	10.5	13.6	22.8%
Total	Mean	14.6	35.7	59.1%

The experimental results indicated that the ship dynamic positioning nonlinear model predictive control (NMPC) algorithm based on the Laguerre function designed in this work could overcome the impact of unknown time-varying ocean environmental disturbances under the conditions of input and input rate saturation. It enabled the ship to reach and maintain the desired position while retaining the control performance of the original nonlinear model predictive control algorithm. Additionally, the computational load significantly decreased, ensuring the real-time solution of the algorithm.

5. Conclusions

This paper proposes a novel nonlinear model predictive control (NMPC) algorithm for ship dynamic positioning based on the Laguerre function. The algorithm uses the Laguerre function to describe the control increment signal of the linear system after feedback linearization, reducing the dimensions of the coefficient matrices in the nonlinear constraint problems. This addresses the issue of the high computational load in the original nonlinear model predictive control algorithm. Finally, the algorithm was validated through simulation experiments on a supply ship. The results demonstrated that the improved ship dynamic positioning NMPC algorithm, under input and input rate saturation conditions, overcame the impact of unknown time-varying disturbances, such as wind, waves, and currents. It ensured that the ship reached and maintained the desired position and heading angle. The new algorithm retains the favorable control performance of the original NMPC algorithm while addressing the computational load issue, satisfying real-time computational requirements.

In future work, we will study the stability and reliability of the NMPC algorithm based on the Laguerre function and consider thrust allocation to solve the overdriving problem for dynamic positioning ships.

Author Contributions: Conceptualization, Y.Y.; methodology, Y.Y.; formal analysis, D.G. and X.Q.; software, X.Q. and H.S.; data curation, X.Q.; resources, X.Q.; writing—original draft preparation, X.Q.; writing—review and editing, X.Q. and D.G.; project administration, Y.Y.; funding acquisition, X.Q. and Y.Y. All authors have read and agreed to the published version of the manuscript.

Funding: This research was partially supported by the following: (a) the National Key R&D Program of China (No. 2022YFB4300803, No. 2022YFB4301402) by Ministry of Science and Technology of the People's Republic of China; (b) the 2023 Liaoning Provincial Science and Technology Plan (Key) Project (No. 2023JH1/10400047) by Liaoning Provincial Department of science and technology; and (c) the 2023 Dalian Science and Technology Talent Innovation Support Policy Project (No. 2023RY005) by Dalian Bureau of Science and Technology.

Institutional Review Board Statement: Not applicable.

Informed Consent Statement: Not applicable.

Data Availability Statement: The raw data supporting the conclusions of this article will be made available by the authors on request.

Conflicts of Interest: Author Xiaobin Qian was employed by the company Zhilong (Dalian) Marine Technology Co., Ltd. The remaining authors declare that the research was conducted in the absence of any commercial or financial relationships that could be construed as a potential conflict of interest

References

1. Sørensen, A.J. A survey of dynamic positioning control systems. *Annu. Rev. Control* **2011**, *35*, 123–136. [[CrossRef](#)]
2. Fossen, T.I. *Handbook of Marine Craft Hydrodynamics and Motion Control*; Wiley: Hoboken, NJ, USA, 2011.
3. Bian, X.Q.; Fu, M.Y.; Wang, Y.H. *Ship Dynamic Positioning*; Science Press: Beijing, China, 2011.
4. Shi, Y.; Shen, C.; Fang, H.; Li, H. Advanced control in marine mechatronic systems: A survey. *IEEE/ASME Trans. Mechatron.* **2017**, *22*, 1121–1131. [[CrossRef](#)]
5. Perez, T.; Donaire, A. Constrained control design for dynamic positioning of marine vehicles with control allocation. *Model. Identif. Control* **2009**, *30*, 32–46. [[CrossRef](#)]
6. Fossen, T.I.; Perez, T. Kalman filtering for positioning and heading control of ships and offshore rigs. *IEEE Control Syst. Mag.* **2009**, *29*, 32–46.
7. Fung, P.T.-K.; Grimbé, M. Dynamic ship positioning using self-tuning Kalman filter. *IEEE Trans. Autom. Control* **1983**, *28*, 339–349. [[CrossRef](#)]
8. Zhang, Y.H.; Jiang, J.G.; Gao, D.K. Novel disturbance compensating dynamic positioning of dredgers based on adaptive backstepping. *J. Southeast Univ. (Eng. Ed.)* **2011**, *6*, 680–688.
9. Muhammad, S.; Dòria-Cerezo, A. Passivity-based control applied to the dynamic positioning of ships. *IET Control Theory Appl.* **2012**, *6*, 680–688. [[CrossRef](#)]
10. Fossen, T.I.; Grøvlén, A. Nonlinear output feedback control of dynamically positioned ships using vectorial observer backstepping. *IEEE Trans. Control Syst. Technol.* **1998**, *6*, 121–128. [[CrossRef](#)]
11. Du, J.L.; Hu, X.; Krstić, M.; Sun, Y.Q. Robust dynamic positioning of ships with disturbances under input saturation. *Automatica* **2016**, *73*, 207–214. [[CrossRef](#)]
12. Tannuri, E.A.; Agostinho, A.C.; Morishita, H.M.; Moratelli, L. Dynamic positioning systems: An experimental analysis of sliding mode control. *Control Eng. Pract.* **2010**, *18*, 1121–1132. [[CrossRef](#)]
13. Do, K.D. Global robust and adaptive output feedback dynamic positioning of surface ships. *J. Mar. Sci. Appl.* **2011**, *10*, 325–332. [[CrossRef](#)]
14. Hassani, V.; Sørensen, A.J.; Pascoal, A.M.; Athans, M. Robust Dynamic Positioning of offshore vessels using mixed- μ synthesis modeling, design, and practice. *Ocean Eng.* **2017**, *129*, 389–400. [[CrossRef](#)]
15. Yang, Y.; Guo, C.; Du, J.L. Robust adaptive NN-based output feedback control for a dynamic positioning ship using DSC approach. *Sci. China (Inform. Sci.)* **2014**, *57*, 1–3. [[CrossRef](#)]
16. Zhang, G.Q.; Lv, S.N.; Huang, C.F.; Zhang, X.K. Robust adaptive control for dynamic positioning vehicles in presence of adjustable threshold rule and input constraints. *Ocean. Eng.* **2023**, *282*, 114950. [[CrossRef](#)]
17. Cho, S.; Shim, H.; Kim, Y.A. Dynamical Sliding Mode Control for Robust Dynamic Positioning Systems of FPSO Vessels. *J. Mar. Sci. Eng.* **2022**, *10*, 474. [[CrossRef](#)]
18. Xi, Y.G.; Li, D.W.; Lin, S. Model Predictive Control—Status and Challenges. *Acta Autom. Sin.* **2013**, *39*, 222–236. [[CrossRef](#)]
19. Wang, Y.H.; Shi, X.C.; Bian, X.Q. Restriction control of marine dynamic positioning system based on model predictive control. *Ship Eng.* **2007**, *29*, 22–25.
20. Wang, Y.H.; Sui, Y.F.; Wu, J. Marine dynamic position system based on nonlinear model predictive control. *J. Harbin Eng. Univ.* **2013**, *34*, 110–115.
21. Veksler, A.; Johansen, T.A.; Borrelli, F.; Realfsen, B. Dynamic Positioning with Model Predictive Control. *IEEE Trans. Control Syst. Technol.* **2016**, *24*, 1340–1353. [[CrossRef](#)]
22. Gierusz, W.; Miller, A. Prediction Control Systems in Marine Applications. *Int. J. Mar. Navig. Saf. Sea Transp.* **2020**, *14*, 361–366. [[CrossRef](#)]
23. Miller, A. Model predictive ship trajectory tracking system based on line of sight method. *Bull. Pol. Acad.-Sci.-Tech. Sci.* **2023**, *71*, e145763. [[CrossRef](#)]

24. Wang, L.P. *Model Predictive Control System Design and Implementation Using MATLAB*; Springer-Verlag London Limited: London, UK, 2009.
25. Kong, X.B.; Liu, X.J. Continuous-time nonlinear model predictive control with inputoutput linearization. *Control Theory Appl.* **2012**, *29*, 217–224.
26. Fossen, T.I.; Sagatun, S.I.; Sørensen, A.J. Identification of dynamically positioned ships. *Control Eng. Pract.* **1996**, *4*, 369–376. [[CrossRef](#)]

Disclaimer/Publisher’s Note: The statements, opinions and data contained in all publications are solely those of the individual author(s) and contributor(s) and not of MDPI and/or the editor(s). MDPI and/or the editor(s) disclaim responsibility for any injury to people or property resulting from any ideas, methods, instructions or products referred to in the content.